Metabolism Clinical and Experimental 99 (2019) 90–101

Contents lists available at ScienceDirect

Metabolism Clinical and Experimental

journal homepage: www.metabolismjournal.com

Hepatic deficiency of Poldip2 in type 2 diabetes modulates lipid and glucose homeostasis

Zhengxuan Jiang [a,1], Jielin Zhou [b,1], Tao Li [b,1,2], Mengjun Tian [b], Jing Lu [b], Yajing Jia [b], Guangming Wan [c,*], Keyang Chen [a,b,**]

[a] Department of Ophthalmology, Second Affiliated Hospital, Anhui Medical University, Hefei, Anhui, China
[b] Department of Nutrition and Food Science, Anhui Medical University School of Public Health, Hefei, Anhui, China
[c] Department of Ophthalmology, First Affiliated Hospital, Zhengzhou University, Zhengzhou, Henan, China

ARTICLE INFO

Article history:
Received 3 July 2019
Accepted 5 July 2019

ABSTRACT

Moderate or low level hydrogen peroxides has been shown to play an important role in vascular smooth muscle cell (VSMC) function, in which the polymerase DNA-directed interacting protein 2 (Poldip2), functioned as a key regulator of NOX4 activity.

In current study, we unexpectedly found that type 2 diabetes mellitus (T2DM) substantially suppresses the hepatic Poldip2 expression, and that the hepatic deficiency of Poldip2 may be correlated with dysregulation of hepatic cholesterol and plasma triglycerides. In cultured hepatocytes, we found that both insulin and leptin may inhibit hepatic expression of Poldip2 under high glucose concentration, but these suppressions were totally abolished under normoglycemic condition. *POLDIP2* siRNA knockdown significantly impaired the H_2O_2 induction by insulin or leptin under normoglycemic condition, contributing the accumulation of cholesterol in cultured liver cells. The *in vivo* restoration of hepatic Poldip2 expression in T2DM mice remarkably rescued the moderate H_2O_2 generation in livers *versus* control mice, resulting in significant amelioration of hepatic cholesterol accumulation and plasma triglyceride levels. Importantly, the moderate induction of H_2O_2 in livers dramatically improved the hepatic PI3K-C_1/AKT signaling or dampened PI3K-$C_2\gamma$/AKT signaling through suppression of PTEN and PTP1B activities, thereby inhibiting the hepatic expression of HMGCR and SREBP2 for cholesterol synthesis. Moreover, the restitution of hepatic Poldip2 expression in diabetic mice significantly lowered the VLDL-cholesterol production rate, and substantially suppressed PEPCK and G6Pase expressions for gluconeogenesis, thus significantly improving the plasma insulin and glucose levels, and ITT and GTT outcomes in diabetic mice. Our findings suggest that hepatic dysregulation of Poldip2 may contribute to diabetic dyslipidemia and hyperglycemia.

1. Introduction

Reactive oxygen species (ROS) are the products of normal cell metabolism and well recognized to play a dual role as both deleterious and beneficial species [1]. The harmful effects of ROS may cause potential biological damage that termed as "oxidative stress" [2–4]. This occurs in biological systems when there is an overproduction of ROS on one side and a deficiency of enzymatic and non-enzymatic antioxidants on the other [5–7]. By contrast, the beneficial effects of ROS happen at low/moderate concentrations and involve physiological roles in response to noxia, which shows that ROS within cells may act as secondary messengers in intracellular signaling cascades [8–11]. The delicate balance between beneficial and harmful effects of ROS is a very important aspect of living organisms and is achieved by mechanisms called "redox regulation". The process of "redox regulation" protects living organisms from various oxidative stresses and maintains "redox homeostasis" by controlling the redox status *in vivo* [12].

Abbreviations: ROS, reactive oxygen spices; c-TRLs, cholesterol- and triglyceride-rich remnant lipoproteins; ASCVD, atherosclerotic cardiovascular disease; ANOVA, analysis of variance; apoB, apolipoprotein B; BSA, bovine serum albumin; GAPDH, glyceraldehyde 3-phosphate dehydrogenase; LDL, low-density lipoprotein; mRNA, messenger RNA; qRT-PCR, quantitative real-time reverse-transcription polymerase chain reaction; siRNA, small interfering RNA; T2DM, type 2 diabetes mellitus; VLDL, very low-density lipoprotein.

* Correspondence to: G. Wan, Department of Ophthalmology, First Affiliated Hospital, Zhengzhou University, 1 East Jianshe Road, Zhengzhou, Henan 450052, China.
** Correspondence to: K. Chen, Department of Health Inspection and Quarantine, Anhui Medical University School of Public Health, 81 Meishan Road, Hefei, Anhui 230032, China.
E-mail addresses: fccwangm5@zzu.edu.cn (G. Wan), chenkeyang@ahmu.edu.cn (K. Chen).

[1] Equally contribute to this work.
[2] Current affiliation: Center of Diseases Control and Prevention (CDC) of Anhui Province, Hefei, China.

https://doi.org/10.1016/j.metabol.2019.153948
0026-0495/

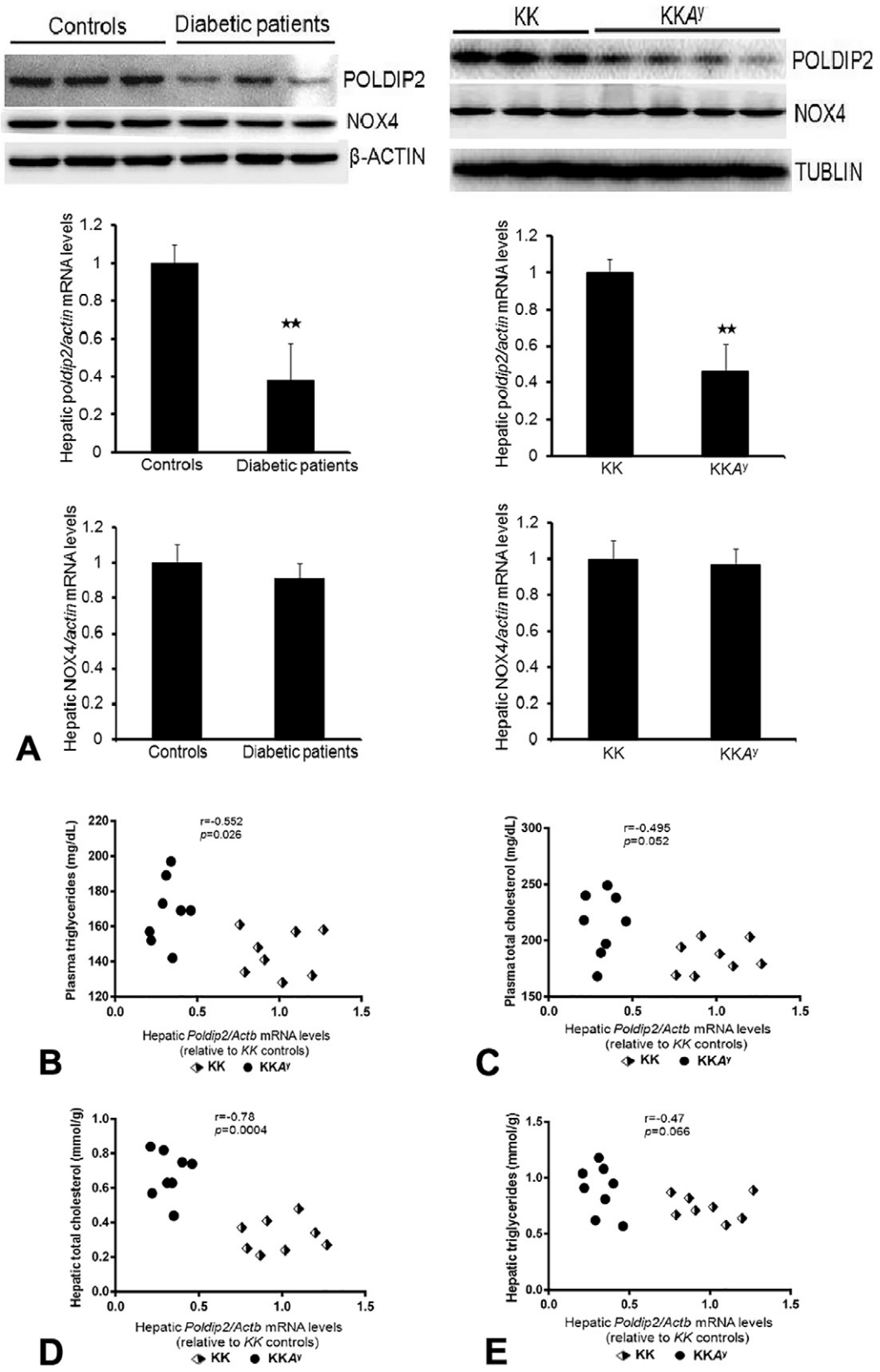

Fig. 1. The inhibition of *POLDIP2* expression both in human and murine diabetic livers is correlated with abnormal lipid contents. Immunoblots of liver tissue homogenates both from human diabetic patients *versus* their controls, and diabetic KK*Ay* mice *versus* KK mice (controls). Each lane represents a single sample from an individual, randomly selected patient or mouse. Poldip2 protein levels were suppressed both in human and murine diabetic livers, while NOX4 protein levels were not changed, which were parallel to the gene transcriptional patterns, mRNA levels normalized to *β-actin*, detected by qRT-PCR in both human and mice. (Mean ± SEM, $n = 3$), $^{**}p < 0.01$ (two-tailed student test). (B) Plot of plasma triglyceride levels *versus* hepatic *POLDIP2* mRNA from the control (◑) and T2DM mice (●). (C) Plot of plasma total cholesterol concentrations *versus* hepatic *POLDIP2* mRNA from the same mice as in (B). (D) Plot of hepatic total cholesterol levels *versus* hepatic *POLDIP2* mRNA from the same mice as in (B). (E) Plot of hepatic triglyceride concentrations *versus* hepatic *POLDIP2* mRNA from the same mice as in (B). All data in this figure are representative of three independent experiments.

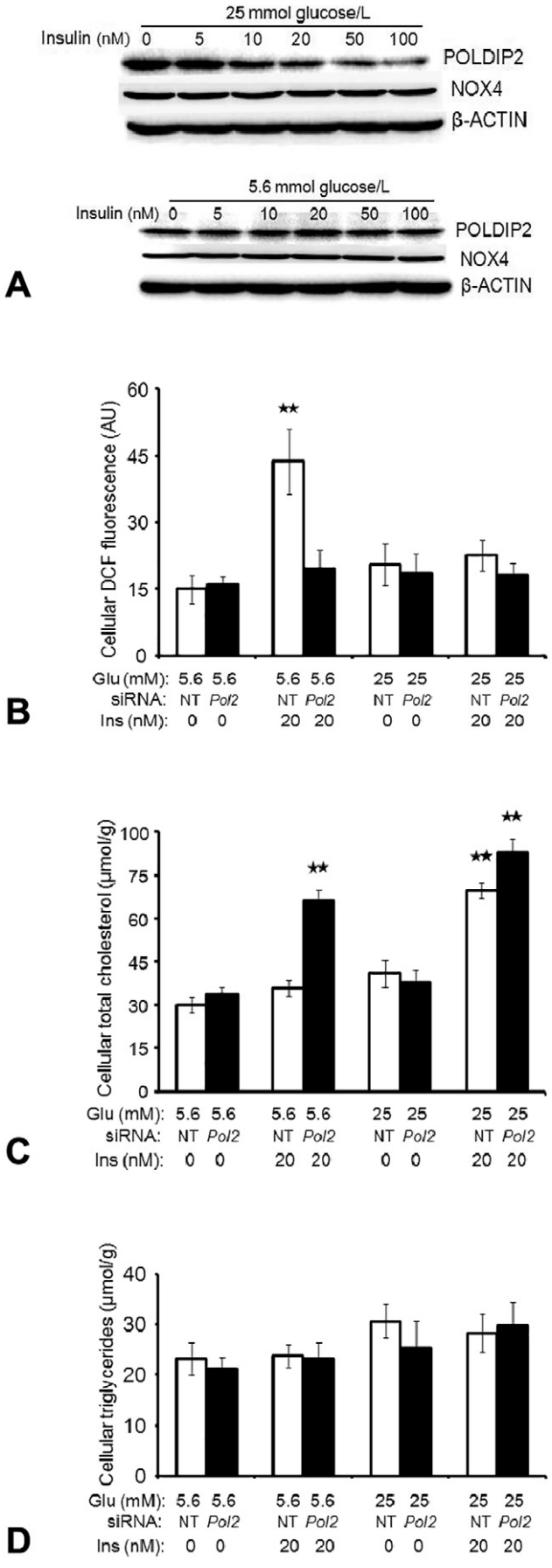

Hydrogen peroxide (H_2O_2) is one of the main ROS and it is generated by the nicotine adenine dinucleotide phosphate (NADPH) oxidases (NOXs) or complex III of the mitochondrial respiratory chain [13,14]. In physiological situations the amount of H_2O_2 is under a tight control to reach the "redox homeostasis" by the peroxiredoxins and glutathione peroxidases as well as by catalase [13]. Particularly, the NOXs-produced H_2O_2 is commonly regarded as signaling-related molecule in normal physiology when it is kept at low/moderate concentration [15,16].

Among the seven NOX homologues found in mammals, the main ROS-producing NOXs in the liver are NOX1, NOX2, and NOX4 [17]. NOX1 and 2 are mainly producing superoxide ($O_2^{\bullet -}$) whereas NOX4 directly produces H_2O_2. NOX4 is a constitutively active membrane-bound isoform and associates with $p22^{phox}$ [18]. Thus interaction between the subunits is an important determinant of enzyme activity [19]. Intriguingly, a novel NOX4 associated partner, namely polymerase (DNA-directed) delta interacting protein 2 (Poldip2), was discovered a decade ago, which functions as an important regulator of NOX4 activity involving the development of cardiovascular disease [20,21]. Poldip2 was initially found to locate in the cellular nucleus and interact with p50 subunit of DNA polymerase and proliferating cell nuclear antigen, which suggested that it might play a role *in vivo* in the processes of DNA replication and DNA repair in the nucleus [22,23]. However, the additional functions of Poldip2, particularly the ones in diabetes, lipid and glucose metabolism are still unknown so far.

In the present study, we unexpectedly found that type 2 diabetes mellitus (T2DM) in human and mice substantially inhibits the hepatic expression of Poldip2 protein, and that suppression of Poldip2 resulted in significant deficiency of signaling-related H_2O_2 production in liver, thereby markedly enhancing the hepatic increase in cholesterol and plasma elevation of triglycerides.

2. Methods

2.1. Human subjects

Normal controls were the 24 patients with gastric cancer. 36 diabetic patients were persons with gastric cancer and diabetes. Liver biopsy was taken during curative surgery. The human study was conducted according to the guidelines of the declaration of Helsinki. The consent forms were signed by patients and the protocol was approved by the clinical research ethics committee of Anhui Medical University. The demographic characteristics please refer to Table 2.

2.2. Type 2 diabetes mice

Hyperphagic, centrally obese, type 2 diabetic KKA^y (KK.Cg-A^y/J) male mice and nondiabetic, phenotypically lean, control KK (a/a

Fig. 2. Suppression of Poldip2 protein expression in cultured liver cells by insulin plus high glucose contributes the deficiency of basal and signaling-functional H_2O_2, thereby eliciting high level of cellular cholesterol. Shown are immunoblots indicating that under high glucose condition (25 mmol/L), insulin inhibits Poldip2 protein levels by cultured McArdle hepatoma cells in a dose-responsive manner, while this effect is disappeared in the cells maintained with normal glucose (5.6 mmol/L). By contrast, the NOX4 protein levels were not affected in both conditions. (B) As described in the Methods section, the McArdle cells maintained in high glucose or normal glucose were seeded in 12-well plate and incubated with corresponding media as indicated. After *POLDIP2* siRNA or nontarget siRNA treatment, bovine insulin was added into media for 5 min. The H_2O_2 level was detected by addition of 10 μM CM-H_2DCF-DA for 10 min. The displayed are the cellular DFC fluorescence representing the basal generation of H_2O_2, under high glucose culture or *POLDIP2*specific siRNA knockdown. (Mean ± SEM, $n = 3$), $^{**}p < 0.001$ (two-tailed student test). (C) The McArdle cells were plated and treated the same as in (B), except that insulin treatment time was increased to 24 h, and no addition of CM-H_2DCF-DA. Shown are the cellular total cholesterol levels, (mean ± SEM, $n = 3$), $^{**}p < 0.01$ (ANOVA). (D) The McArdle cells were plated and treated the same as in (C). Shown are the cellular triglyceride levels, [mean ± SEM, $n = 3$; p value not significant (ANOVA)]. All data in this figure are representative of three independent experiments, respectively.

background) littermates were purchased from Jackson Laboratory (Bar Harbor, ME) and studied at 10 weeks of age. The housing unit was maintained at constant temperature 22–25 °C and 50%–60% relative humidity, with a 12/12-hour light/dark cycle, with free access to tap water. All mice were fed with commercial high-fat (HFD) diet (BEIJING HFK Bio-Technology Co., Ltd., Beijing, China) *ad libitum* for 2 weeks to increase their serum glucose levels. All animals were maintained and used in accordance with the guidelines of the Institutional Animal Care and Use Committee of the Anhui Medical University for Biological and Medical Sciences.

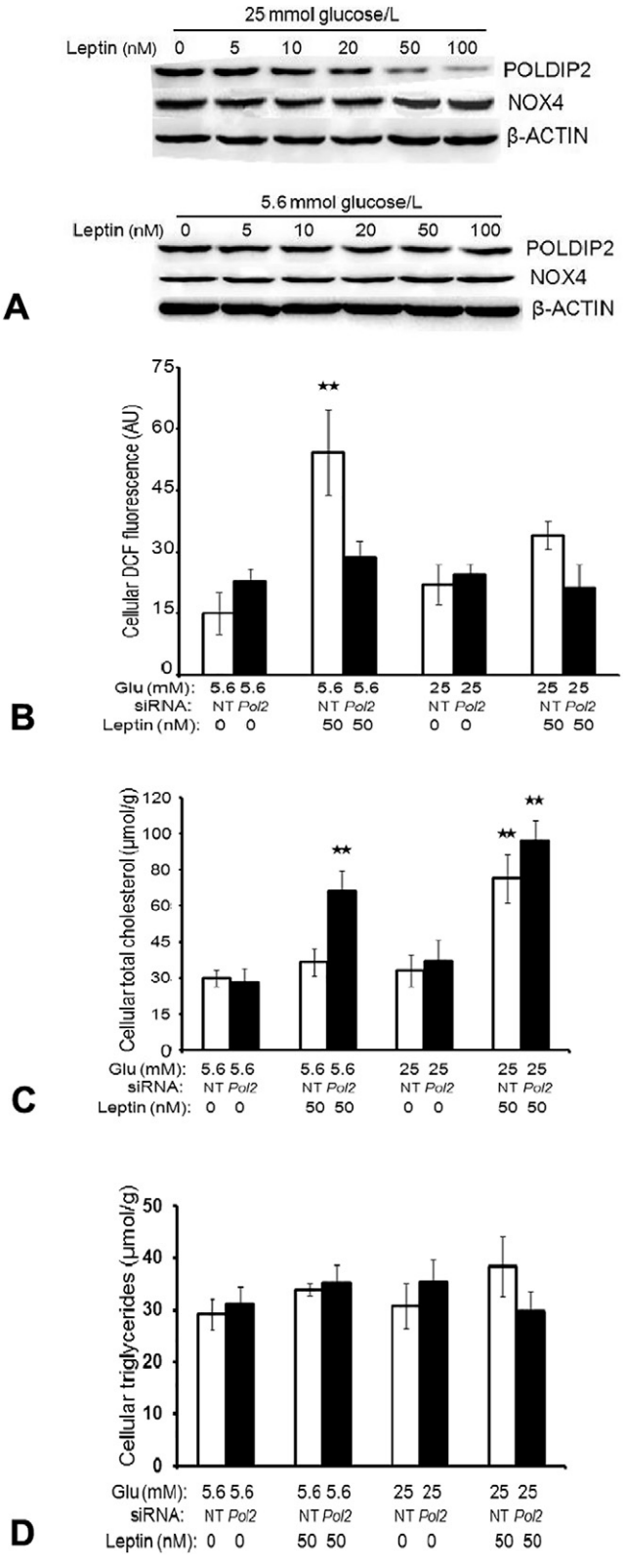

2.3. Biochemical parameters in plasma, hepatoma cells and livers

Serum lipids including total cholesterol (TC), triglyceride (TG), free fatty acid (FFA), high-density lipoprotein (HDL)-cholesterol (HDL—C), and low-density lipoprotein (LDL)-cholesterol (LDL-C), and cellular TC and TG were determined using enzymatic kits (Nanjing Jiancheng Bioengineering Institute, Jiangsu, China) in accordance with the manufacturer's instruction. The lipid levels in murine livers were determined using enzymatic kits (Applygen Technologies Inc., Beijing, China). Insulin and leptin levels in murine plasma were measured by a radioimmunoassay (RIA) kit (Beijing North Institute of Biological Technology, Beijing, China). ApoC-III in murine plasma was detected by Elabscience kit. PTP1B activity was determined by Millipore kit. All measurements were performed in triplicate.

2.4. Immunoblotting

Cellular and liver tissue extractions, immunoblots, were performed following our published protocols [21,30]. Briefly, livers or cells were homogenized in ice-cold lysis buffer containing phosphatase inhibitors. Obtained bands were quantified using Image Software. The different membranes were respectively incubated with antiserum against POLDIP2, NOX4, AKT, p-AKT, PI3K, p-PI3K, PI3KC2-γ, PTEN, p-PTEN, FOXO1, p-FOXO1, SEREBP2, HMGCR and PEPCK, G6Pase, *etc.*

2.5. Cell culture

McA-RH 7777 (McArdle) rat hepatoma cells were cultured as previously described [21,30], and typically maintained in medium with a high glucose concentration (DMEM with 25 mmol/L glucose). For the detection of glucose effect, the cells were incubated in 5.6 mmol/L for 3–4 weeks (media was replaced every 12 h and media glucose level was monitored by glucometer), and then used to compare with those maintained in 25 mmol/L all the times. For insulin treatment, the McArdle cells that were maintained in high glucose media, or in normal glucose media, were seeded in two 6-well plates, respectively. After the cells reach confluence, the cells were washed by PBS three times and then incubated with corresponding fresh high glucose media or normal glucose media containing 2% FBS, respectively. The bovine insulin at different concentrations (0, 5, 10, 20, 50, 100 nM) were added into media. After 24 h incubation, the cells were harvested and the proteins were prepared for immunoblotting.

Fig. 3. Under high glucose milieu, leptin inhibited Poldip2 protein expression in cultured liver cells, and resulted in the abnormal cellular cholesterol content that is related to the absence of signaling-functional H_2O_2. McArdle cells maintained in high glucose or normal glucose were seeded in two 6-well plates and incubated with corresponding media. (A) Leptin at different concentrations as indicated in figure were added in to media and incubated for 24 h. The displayed are immunoblots showing that leptin starting at 20 nmol/ml with high glucose concentration significantly suppresses the Poldip2 protein levels in a dose-dependent manner. The inhibition was abrogated in the cells maintained in 5.6 mmol/L glucose media. The NOX4 protein levels were not changed in both conditions. (B) The same cells as in (A) were seeded in 12-well plate and incubated with corresponding media. After *POLDIP2* siRNA or nontarget siRNA treatment, 50 nmol/ml leptin were added into media and incubated for 24 h. The H_2O_2 level was detected by addition of 10 μM CM-H_2DCF-DA for 10 min. The displayed are the cellular DFC fluorescence representing the basal generation of H_2O_2, under normal or high glucose culture or *POLDIP2* specific siRNA knockdown. (Mean ± SEM, $n = 3$), $^{**}p < 0.01$ (ANOVA). (C) The McArdle cells were plated and treated the same as in (B), without addition of fluorescence reagent. Shown are the cellular total cholesterol levels, (mean ± SEM, $n = 3$–4), $^{**}p < 0.01$ (ANOVA). (D) McArdle cells were plated and treated the same as in (C). Displayed are the cellular triglyceride levels, [mean ± SEM, $n = 3$; p value not significant (ANOVA)]. All data in this figure are representative of three independent experiments, respectively.

For leptin treatment, the McArdle cells were seeded and grown in two 6-well plates by the same way as above insulin treatment. The different concentrations of leptin at 0, 5, 10, 20, 50, 100 nmol/ml were administrated into two 6-well plates with fresh high glucose or normal glucose media containing 2% FBS, respectively. After 24 h incubation, the cells were harvested and the proteins were prepared for immunoblotting.

2.6. siRNA knockdown and function analysis

The fresh McArdle cells were seeded in 24-well plates, including 12 wells with high glucose media and 12 wells with normal glucose media. The cells were incubated at 5% CO_2 and 37 °C overnight. The *POLDIP2* siRNA and nontarget siRNA were added into cells in different wells

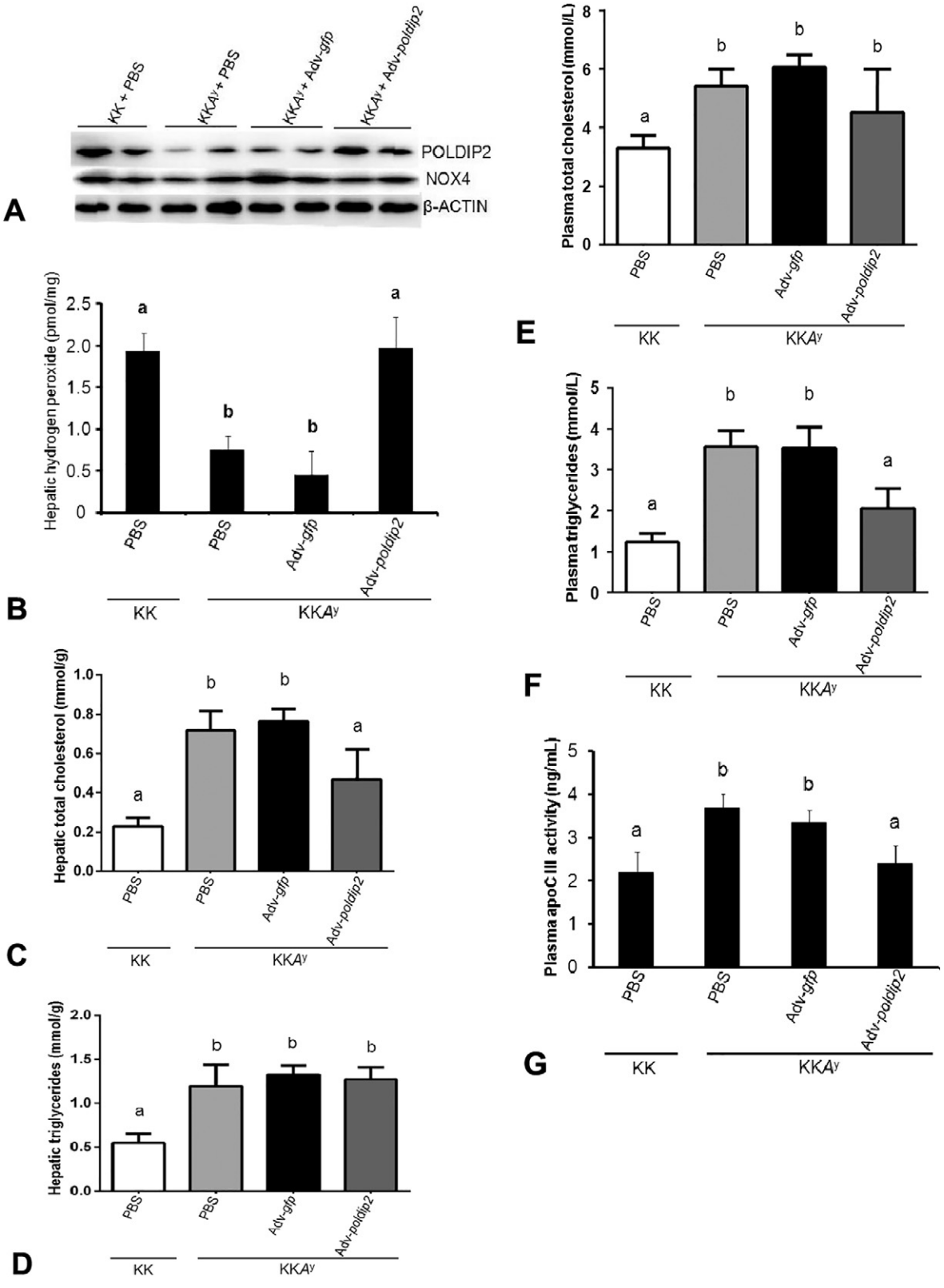

according to the manufacturing's instruction. After 24 h, the cells were incubated with fresh high glucose or normal glucose media containing 10% FBS, respectively. After 48 h incubation, the cells were washed by PBS three times, and incubated with fresh high glucose media or normal glucose media, respectively, containing 2% FBS. The 0, 20 nM insulin, or 0, 50 nmol/ml leptin, were added into different wells, respectively, as indicated in Fig. 2 or 3. After 24 h, the cells were harvested and lyzed for total cholesterol and triglyceride detections by using the kits according to the manufacturing's protocol.

2.7. Hydrogen peroxide determinations

For monitoring intracellular H_2O_2, the McArdle cells were grown in 24-well plates with high glucose or normal glucose media and subject to *POLDIP2* siRNA treatments as described in above function analysis. After 48 h siRNA knockdown, the serum starved cells were left unstimulated or stimulated with 20 nM insulin for 5 min, or with 50 nmol/ml leptin for 24 h, and 10 μM CM-H_2DCF-DA was added into cells for 10 min. CM-H_2DCF-DA is a non-polar compound that readily diffuses into cells, where it is hydrolyzed to the non-fluorescent polar derivative H_2DCF that remains trapped within cells. Intracellular H_2O_2 was detected by the oxidation of H_2DCF and the formation of the fluorescent derivative DCF (2,7-dichlorofluorescein). Fluorescence was monitored using an epifluorescence microscope and quantified using a BMG FLUOstar fluorescent plate reader at an excitation of 488 nm and an emission of 520 nm.

H_2O_2 levels in liver tissue extracts were determined using the Amplex™ Red hydrogen peroxide assay kit based on the manufacturer's instructions. Briefly, liver were mechanically homogenized in ice cold lysis buffer (50 mM Tris [pH 7.4], 1% (v/v) Triton X-100, 150 mM NaCl), clarified by centrifugation (1000 ×*g*, 10 min, 4 °C) and the resulting supernatants processed for H_2O_2 determination and normalized to the corresponding protein content or volume of the sample.

2.8. Hepatic expression of Poldip2 in vivo and VLDL production

To drive expression of wild-type poldip2 protein or GFP protein in livers of KK*A*^{y} mice *in vivo*, mice at 10 weeks of old were divided into 4 groups as indicated in Fig. 4. Adenoviruses were administrated *via* caudal vein injection (10^9 pfu/mouse/week). Mice were studied four weeks after adenoviral injection. For assessments of biochemical characteristics in plasma and of hepatic protein and mRNA, 6 h fasted mice from 4 groups were euthanized, blood samples were collected from the orbital venous plexus and their livers were flushed with cold phosphate-buffered saline before preparing tissue extracts.

For Triton WR-1339 test, the 5 groups of mice (KK + PBS, KK*A*^{y} + Adv-gfp, KK*A*^{y} + Adv-gfp + Triton WR1339, KK*A*^{y} + Adv-*poldip2*, KK*A*^{y} + Adv-*poldip2* + Triton WR1339), were injected with Adv-*poldip2* or Adv-gfp viruses or PBS exactly same as described above. After 4 weeks of virus injection, the third and fifth groups of mice were *iv* injected with Triton WR-1339 (500 mg/kg) after 4 h of fasting. Immediately prior to Triton injection, and at 20, 40, 60, 90 and 120 min following Triton injection, blood samples were drawn in heparin capillary tubes, plasma was prepared, the each VLDL fraction from 200 μl plasma was isolated by ultracentrifugation (d < 1.006 ×*g*/ml), and VLDL-TG and -TC levels were determined by the enzymatic kits.

2.9. ITT and GTT experiments

The mice with hepatic *in vivo* expression of Poldip2 protein or GFP protein as aforementioned, were used for Insulin tolerance test (ITT) and glucose tolerance test (GTT). The experiments were performed on 6–8 h fasted conscious mice respectively by injecting bovine insulin (0.7 mU/g body weight) into the intraperitoneal cavity and measuring glucose in tail blood immediately before and 20, 40, 60, 80, 100 and 120 min after injection using a Accu-Check glucometer. For intravenous GTTs, mice were fasted for 6 h, anesthetized with sodium pentobarbitone and a catheter inserted into the left carotid artery. A bolus of glucose (2 mg/g body weight) was injected into the intraperitoneal cavity and 200 μl of blood was sampled from the carotid artery at 0, 15, 30, 60, 90 and 120 min for plasma glucose analyses. Blood was immediately centrifuged, the plasma was separated and red blood cells resuspended in heparinised saline and reinfused into the animal prior to the collection of the next blood sample. Plasma was frozen for insulin and glucose determinations.

2.10. Statistical analyses

Quantitative data from qRT-PCR, H_2O_2 generation, and plasma and cellular lipids, ITT and GTT, *etc.*, were analyzed using Sigma Plot version 11 (Systat Software Inc.). Normally distributed data are reported as means ± SEMs. For comparisons between a single experimental group and a control, the unpaired, two-tailed *t*-test was used. For comparisons involving several groups simultaneously, ANOVA was initially used, followed by pairwise comparisons using the Student-Newman-Keuls *q* statistic. Differences were considered to be significant for $p \le 0.05$.

3. Results

3.1. T2DM substantially inhibits POLDIP2 expression in liver, which correlates with abnormal levels of hepatic cholesterol and plasma triglycerides

The human liver tissues from control and diabetic patients were collected *via* biopsy as described in Table 2. The murine liver tissues were obtained from control KK and diabetic KK*A*^{y} mice as depicted in the Methods section. The human and murine liver samples were prepared and run by immunoblotting to detect the hepatic protein levels of Polidip2 and NOX4, respectively, in which T2DM in both human and mice dramatically inhibited Poldip2 protein synthesis in livers, while NOX4 protein levels were not significantly changed (Fig. 1A upper panels). Meanwhile, the total RNA samples were prepared from human and murine liver tissues as well. The quantitative RT-PCR was conducted to measure the mRNA levels of *POLDIP2* and *NOX4*. Our data showed that T2DM in both human and mice

Fig. 4. *In vivo* hepatic expression of *POLDIP2* in diabetic KK*A*^{y} mice normalized the protein level, and rescued the signaling-functional H_2O_2, and therefore substantially alleviating high content of cholesterol in liver and high concentration of triglyceride in plasma. Adenoviral particles were injected into KK*A*^{y} mice as described in the Methods section. After 4 weeks of injection, the proteins were extracted from murine livers from the four groups as indicated. (A) Immunoblots are shown for the Poldip2 and NOX4 protein levels, each lane representing the different individual animal. (B) The liver tissue homogenates were prepared from the same mice as in (A). The Amplex™ Red was applied to detect H_2O_2 levels in the liver homogenates from 4 groups of mice. (mean ± SEM, $n = 3$). Columns labeled with different lower case letters (a, b) are statistically different, $p < 0.001$ (Student-Newman-Keuls test). (C) Shown are the hepatic total cholesterol levels by the same samples as in (A). Columns labeled with different lower case letters (a, b) are statistically different, $p < 0.01$ (Student-Newman-Keuls test). (D) Shown are the hepatic triglyceride levels by the same samples as in (A). (Mean ± SEM, $n = 3$), columns labeled with different lower case letters (a, b) are statistically different, $p < 0.01$ (Student-Newman-Keuls test). (E) Displayed are the total cholesterol concentrations in the plasma from the same mice as in (A). (Mean ± SEM, $n = 3$), columns labeled with different lower case letters (a, b) are statistically different, $p < 0.01$ (Student-Newman-Keuls test). (F) Displayed are the triglyceride concentrations in the plasma from the same mice as in (A). (Mean ± SEM, $n = 3$), columns labeled with different lower case letters (a, b) are statistically different, $p < 0.001$ (Student-Newman-Keuls test). (G) Plasma apoC-III activity was shown from the same four groups of mice as in (A). (Mean ± SEM, $n = 3$), columns labeled with different lower case letters (a, b) are statistically different, $p < 0.001$ (Student-Newman-Keuls test). All data in this figure are representative of three independent experiments, respectively.

substantially suppressed *POLDIP2* mRNA levels, while the *NOX4* mRNA levels were not significantly affected (Fig. 1A lower panels), suggesting that the T2DM may dampen hepatic Poldip2 expression in transcription level.

To explore the possible relationship of hepatic *POLDIP2* mRNA levels and hepatic and plasma lipid concentrations, we examined the statistical correlations in control KK and diabetic KK*A*^{y} mice. A plot of plasma triglyceride concentrations *versus* hepatic *POLDIP2* mRNA levels showed significant segregation of control mice in the lower right hand corner from the KK*A*^{y} mice in the upper left hand corner (Fig. 1B). A graph of hepatic *POLDIP2* mRNA levels *versus* plasma total cholesterol concentrations revealed no significant differences between control and diabetic mice (Fig. 1C). Likewise, the plot of hepatic total cholesterol levels *versus* hepatic *POLDIP2* mRNA levels demonstrated complete segregation of control KK from diabetic KK*A*^{y} mice (Fig. 1D). Whereas the graph of hepatic triglyceride levels *versus* hepatic *POLDIP2* mRNA levels showed no significant disparity between control KK and diabetic KK*A*^{y} mice (Fig. 1E). In the cases of Fig. 1B and D, calculated Spearman rank correlation coefficients were statistically significant.

3.2. Insulin suppresses hepatic Poldip2 protein level under high glucose concentration, resulting in loss of signaling-functional H_2O_2 and overproduction of hepatic cholesterol

To seek the metabolic factors regulating hepatic Poldip2 expression, the exogenous insulin was respectively added into the cultured liver cells, McArdle7777 rat hepatocytes, under different glucose concentrations. Displayed were the immunoblotting of Poldip2 and NOX4 proteins in the treated cells, showing that insulin could sharply inhibit the Poldip2 protein synthesis in a dose dependent manner under high glucose concentration (Fig. 2A upper panel), while this suppression could be completely eliminated under normoglycemic state (Fig. 2A lower panel). Meanwhile the NOX4 protein levels were not affected by insulin under either high or low glucose concentration (Fig. 2A). Furthermore, the *POLDIP2* specific siRNA or control siRNA was transfected into the McArdle cells, which were then treated with or without 20 nM insulin. The H_2O_2 levels were detected by the cells, showing that insulin could substantially stimulate the moderate production of H_2O_2 under low glucose concentration, while this enhancement was totally suppressed by knockdown of Poldip2 protein levels (Fig. 2B). Likewise, the high glucose concentration completely blocked the H_2O_2 generation by insulin stimulation as well (Fig. 2B). It is noteworthy that high glucose concentration itself didn't promote or impair the H_2O_2 production in the cultured hepatocytes after 24 h incubation (Fig. S1). In contrary to H_2O_2 levels, the cholesterol productions in the above treated hepatocytes were sharply elevated by suppression of H_2O_2 (Fig. 2C). However, the cellular triglyceride contents were not affected under the same conditions as the aforementioned (Fig. 2D).

3.3. Leptin dampens hepatic Poldip2 protein level under high glucose level, resulting in loss of signaling-functional H_2O_2 and overproduction of hepatic cholesterol

Like hyperinsulinemia, hyperleptinemia in blood is usually regarded as a biomarker for T2DM as well. To explore the leptin role in the regulation of Poldip2 expression in liver, the exogenous leptin was respectively added into the cultured McArdle cells under different glucose concentrations. The Poldip2 and NOX4 protein levels in the treated cells were respectively measured by immunoblotting, indicating that leptin with high glucose concentration (25 mmol/L) could dramatically impair the Poldip2 protein synthesis in a dose-dependent pattern in liver cells (Fig. 3A upper panel), while this inhibition could be completely relieved under normoglycemic state (5.6 mmol/L) (Fig. 3A lower panel). Meanwhile the NOX4 protein levels were not changed by leptin under either high or low glucose concentration (Fig. 3A). Moreover, the *POLDIP2* specific siRNA or control siRNA was transfected into the McArdle cells, which were then treated with or without 50 nM leptin. The H_2O_2 levels were detected by the cells, showing that leptin could markedly stimulate the moderate production of H_2O_2 under low glucose concentration, while this elevation was totally inhibited by knockdown of Poldip2 protein levels (Fig. 3B). Likewise, the high glucose concentration completely blocked the H_2O_2 generation by leptin as well (Fig. 2B). In contrast to H_2O_2 levels, the cholesterol productions in the above treated hepatocytes were sharply enhanced by suppression of H_2O_2 (Fig. 3C). However, the cellular triglyceride contents were not affected under the same conditions as the aforementioned (Fig. 3D).

3.4. In vivo rescue of hepatic Poldip2 level in T2DM mice normalizes the signaling-functional H_2O_2, thus ameliorating the accumulation of hepatic cholesterol and plasma triglyceride levels

To assess the *in vivo* role of Poldip2 in the modulation of lipid metabolism under T2DM state, the murine *POLDIP2* gene coding sequences were packaged into adenovirus particles, which were then injected into T2DM KK*A*^{y} mice *via* tail vein. The hepatic restitution of Poldip2 protein levels were confirmed by the immunoblotting (Fig. 4A). Meanwhile, compared to the healthy controls, the hepatic moderate H_2O_2 production was totally normalized after the rescue of *in vivo* Poldip2 expression (Fig. 4B). Intriguingly, the dramatic elevation of total cholesterol in murine livers by T2DM was completely normalized by the *in vivo* replenishment of Poldip2 protein (Fig. 4C), while the sharp enhancement of hepatic triglyceride by T2DM was not affected (Fig. 4D). In contrast, *in vivo* expression of Poldip2 protein resulted in the normalization of plasma hypertriglyceridemia caused by T2DM (Fig. 4F), which is also consistent with the significant improvement of nonesterified fatty acid levels elicited by replenishment of Poldip2 in T2DM KK*A*^{y} mice (Table 1). Whereas the elevated plasma total cholesterol was not significantly improved by the restitution of Poldip2 in diabetic murine livers (Fig. 4E). Moreover, the drastic increase in apoCIII activity elicited by T2DM was

Table 1
Characteristics of KK*A*^{y} mice treated with Adv-*poldip2*.

Characteristics	KK	KK*A*^{y}			*p* value
	PBS	PBS	Adv-*gfp*	Adv-*poldip2*	
Body weight (g)	28.7 ± 0.3^{a}	34.4 ± 1.0^{b}	37.3 ± 2.4^{b}	35.3 ± 1.1^{b}	<0.001
Glucose (mmol/L)	6.6 ± 0.3^{a}	9.5 ± 0.3^{b}	10.2 ± 1.0^{b}	7.4 ± 0.2^{c}	<0.002
Insulin (pmol/L)	58.2 ± 11.2^{a}	179.2 ± 31.1^{b}	183.4 ± 41.1^{b}	108.4 ± 22.0^{c}	<0.001
HOMA-IR	2.6 ± 0.3^{a}	10.8 ± 1.1^{b}	11.5 ± 1.4^{b}	5.1 ± 0.6^{c}	<0.001
Leptin (ng/mol)	1.9 ± 0.9	1.9 ± 1.0	3.1 ± 0.5	1.9 ± 0.6	>0.05
Nonesterified-fatty acid (mmol/L)	0.65 ± 0.2^{a}	1.1 ± 0.4^{b}	1.4 ± 0.5^{b}	0.71 ± 0.2^{a}	<0.001

All data are presented as the mean ± SEM (ANOVA), $n = 6$–8 mice/group. For each characteristic, any two numbers labeled with the same lowercase letter (a, b, c) are statistically indistinguishable. If two numbers do not share a lowercase letter, they are statistically different [$p < 0.01$, (Student-Newman-Keuls *post hoc* pairwise test)].

Table 2
Inclusion of human subjects for observational study.

Characteristics	Participants	
	Controls	Diabetic patients
Race	Han Chinese	Han Chinese
Location	Hefei, China	Hefei, China
Gender	Male	Male
Body weights (kg)	50–70	65–75
Age	53–78	50–75
Hypertension (mmHg)	No or border line (≤140/90)	No or border line (≤140/90)
Smoking	No	No
Gastric or colorectal cancer	Yes	Yes
FPG (mmol/L)	5.35–6.07	7.12–11.58
Plasma TG (mmol/L, mean ± SE, n = 26–32)	1.67	2.75
Medication history	No	No

At the time of submission of this manuscript, the total number of participants recruited for the liver tissue biopsy was 58, including 26 controls and 32 diabetic patients based on the criteria listed in the table above. The human subjects who had some preexisting diseases or medication history, except the diabetes and newly diagnosed gastric or colorectal cancers, were excluded from the sampling. The representative tissue samples for Immunoblotting and qRT-PCR were randomly picked up from the total collection of 58. The Immunoblots and qRT-PCR shown in Fig. 1A (left side) were the representatives of three independent experiments, respectively, for the human liver tissues. In addition, due to the very limited amount of liver tissues by biopsy, other assays, like co-ip, immunohistochemistry *etc.*, could not be conducted. Other conditions were described in the "Materials and methods" section.

totally normalized by *in vivo* expression of Poldip2 protein (Fig. 4G), suggesting the promoted degradation of plasma triglyceride *via* enhanced lipoprotein lipase (LpL) activity.

3.5. In vivo expression of hepatic Poldip2 improves the PI3K/AKT signaling pathway, and suppresses the hepatic cholesterol synthesis|

In order to explore the NOX4-Poldip2 mediated relief of insulin resistance caused by T2DM, the liver samples from the adenovirus infected KK*A*^{y} mice mentioned in Fig. 4 were prepared, and the displayed are the detections of key components of insulin signaling pathway by immunoblotting. We found that the hepatic phosphorylation levels of PI3K and AKT were dramatically enhanced respectively by the replenishment of Poldip2 protein *in vivo* (Fig. 5A), indicating the normalization of insulin sensitivity. In addition, the previous study [24] suggested that PI3KC2γ could still promote the AKT activity by phosphorylating itsThr308, thus contributing to the lipogenesis under T2DM state. Here, our data revealed that *in vivo* expression of *POLDIP2* could normalize the elevated PI3KC2γ proteins induced by T2DM (Fig. 5B). Furthermore, the drastic elevations of HMGCR and SREBP2 proteins by T2DM were also substantially inhibited (Fig. 5C), demonstrating the marked suppression of

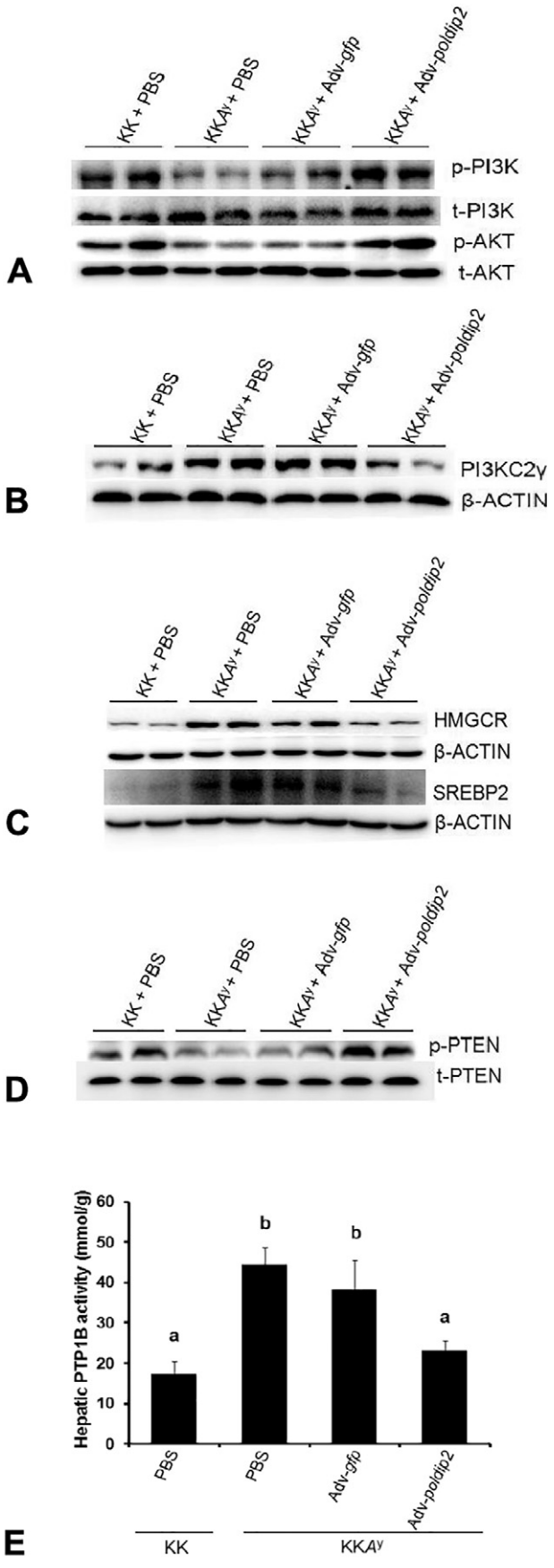

Fig. 5. Hepatic replenishment of Poldip2 protein in diabetic KK*A*^{y} mice ameliorates the insulin signaling and suppresses the cholesterol synthesis in liver, *via* inhibition of PTEN and PTP1B activities. Type 2 diabetic KK*A*^{y} mice were injected with the adenoviral particles containing wild type *POLDIP2* or *gfp* as described in Fig. 4. The proteins were extracted from the livers of four groups of mice. (A) Shown are the phosphorylation levels of PI3K and its total protein levels in the four groups. The phosphorylation levels of AKT and its total protein levels were displayed as well. (B) Immunoblots are shown the protein levels of PI3KC2-γ after *in vivo* hepatic expression of Poldip2 in diabetic KK*A*^{y} mice. (C) Displayed are the protein levels of HMGCR and SREBP2, respectively. Both of them are related to cholesterol synthesis. (D) Shown are the phosphorylation levels of PTEN and its total proteins for the four groups of mice. (E) Hepatic PTP1B activity was detected for four groups of mice. (Mean ± SEM, $n = 3$), columns labeled with different lower case letters (a, b) are statistically different, $p < 0.001$ (Student-Newman-Keuls test). All data in this figure are representative of three independent experiments, respectively.

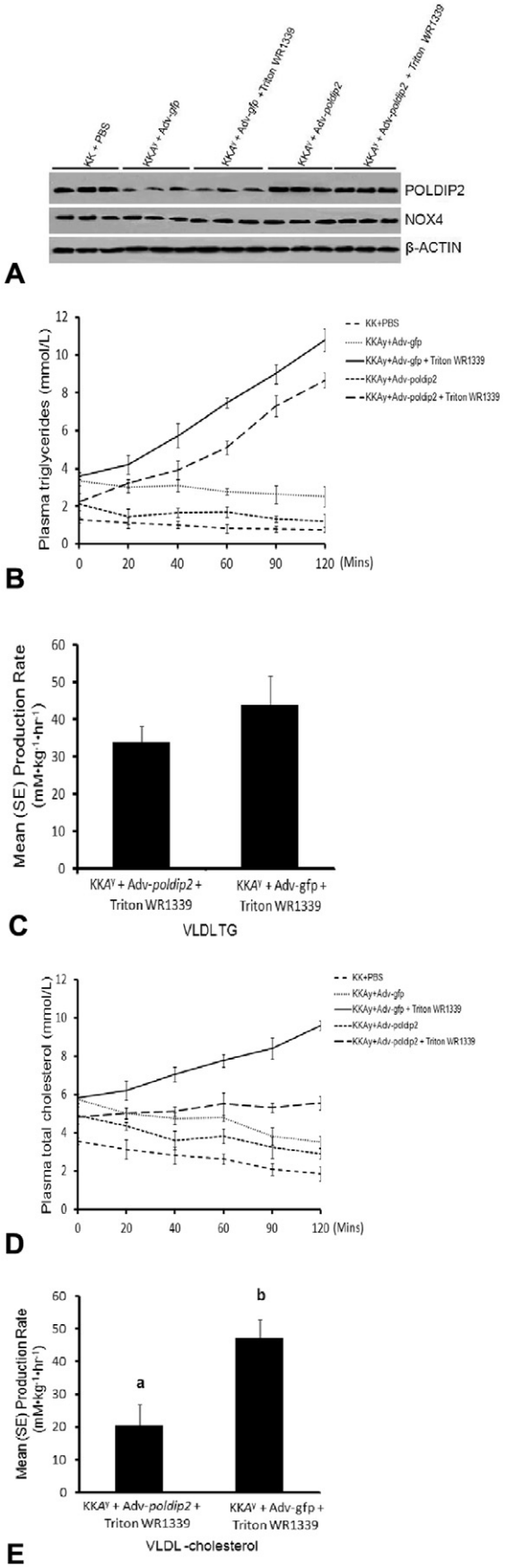

cholesterol synthesis, consistent with the effects in Fig. 4C. Based on the published literature, the PTPase family including the PTEN and PTP1B are the main targets of H_2O_2 [25]. We found that hepatic moderate generation of H_2O_2 induced by the restitution of Poldip2 *in vivo* sharply phosphorylated the PTEN proteins in diabetic livers (Fig. 5D), suggesting the drastic inhibition of PTEN activity. Likewise, the enhanced PTPIB activity by T2DM was also normalized by the *in vivo* expression of Poldip2 (Fig. 5E), indicating the dramatic improvement of insulin signaling.

3.6. In vivo rescue of hepatic Poldip2 level in T2DM mice ameliorates VLDL-cholesterol production rate

To address the impact of *in vivo* rescue of hepatic Poldip2 on VLDL-triglyceride and VLDL-cholesterol productions, the *in vivo* injection of Triton WR1339 in KK*A*^{y} mice was used to examine the plasma triglyceride and cholesterol levels through inhibition of LpL activity. As described in Fig. 4A, the KK*A*^{y} mice were infected with Adv-*POLDIP2* or Adv-gfp viruses *via* tail vein injection. After 4 weeks of injection, 500 mg/kg Triton WR1339 was *iv* injected into one group of 4 h fasted KK*A*^{y} mice infected Adv-gfp or Adv-*POLDIP2*. We found that the suppression of hepatic Poldip2 protein levels induced by T2DM was completely normalized by *in vivo* restitution of Adv-*POLDIP2* in diabetic murine livers compared to the healthy controls, and this elevation was not affected by the injection of Triton WR1339 (Fig. 6A). Furthermore, the plasma triglyceride levels from five groups of mice were measured based on the different time points immediately before and after detergent or PBS injection. The lipid excursion shows that *in vivo* restoration of Poldip2 markedly lowered the plasma triglyceride levels compared to the group of KK*A*^{y} mice infected with Adv-gfp (Fig. 6B), which is also consistent with the result in Fig. 4F. However, after the detergent injection, the increase rates of plasma VLDL-triglyceride were similar between two groups of KK*A*^{y} mice infected with Adv-gfp and Adv-*POLDIP2*, suggesting that *in vivo* hepatic restoration of Poldip2 in KK*A*^{y} mice did not significantly raise the hepatic production rate of VLDL-triglyceride in KK*A*^{y} mice compared to the control mice with *in vivo* expression of gfp (Fig. 6C). Meanwhile, the plasma cholesterol levels were measured in the same samples as described in Fig. 6B. Shown here are the cholesterol excursion curves (Fig. 6D), indicating that *in vivo* rescue of hepatic Poldip2 did not significantly lower the plasma cholesterol levels compared to the *in vivo* expression of gfp. Nevertheless, the replenishment of hepatic Poldip2 sharply mitigated the hepatic VLDL-cholesterol generation rate, comparing with that in the group of KK*A*^{y} mice with hepatic gfp expression (Fig. 6E).

3.7. In vivo expression of hepatic Poldip2 significantly inhibits hepatic gluconeogenesis and improves insulin sensitivity

Based on the previous literature, phosphorylation of Ser473 in AKT protein is responsible for the inhibition of FoxO1 activity

Fig. 6. *In vivo* hepatic expression of *POLDIP2* in diabetic KK*A*^{y} mice remarkably reduced the VLDL production rate. Type 2 diabetic KK*A*^{y} mice were injected with the adenoviral particles containing wild type *POLDIP2* or *gfp* as described in Fig. 4. After four weeks of injection, the mice were fasted for 4 h, and then one group of KK*A*^{y} mice injected with Adv-gfp or Adv-poldip2 were given Triton WR-1339 (500 mg/kg). (A) The liver tissue homogenates were prepared from the five groups of mice. Shown are the immunoblots for Poldip2 and NOX4 protein levels. (B) The blood was collected from five groups of mice at indicated time points during the treatment procedure. Plasma triglycerides were detected and shown as different curves. (C) The production rates of the VLDL-triglycerides were calculated for two groups of mice treated with the detergent. (D) The VLDL from the murine plasma collected as in (B) was assayed for total cholesterol and displayed in different curves for five groups of mice. (E) The production rates of the VLDL-cholesterol were calculated for two groups of mice treated with Triton WR1339. Columns labeled with different lower case letters (a, b) are statistically different, $p < 0.001$ (Student-Newman-Keuls test). All data in this figure are representative of three independent experiments, respectively.

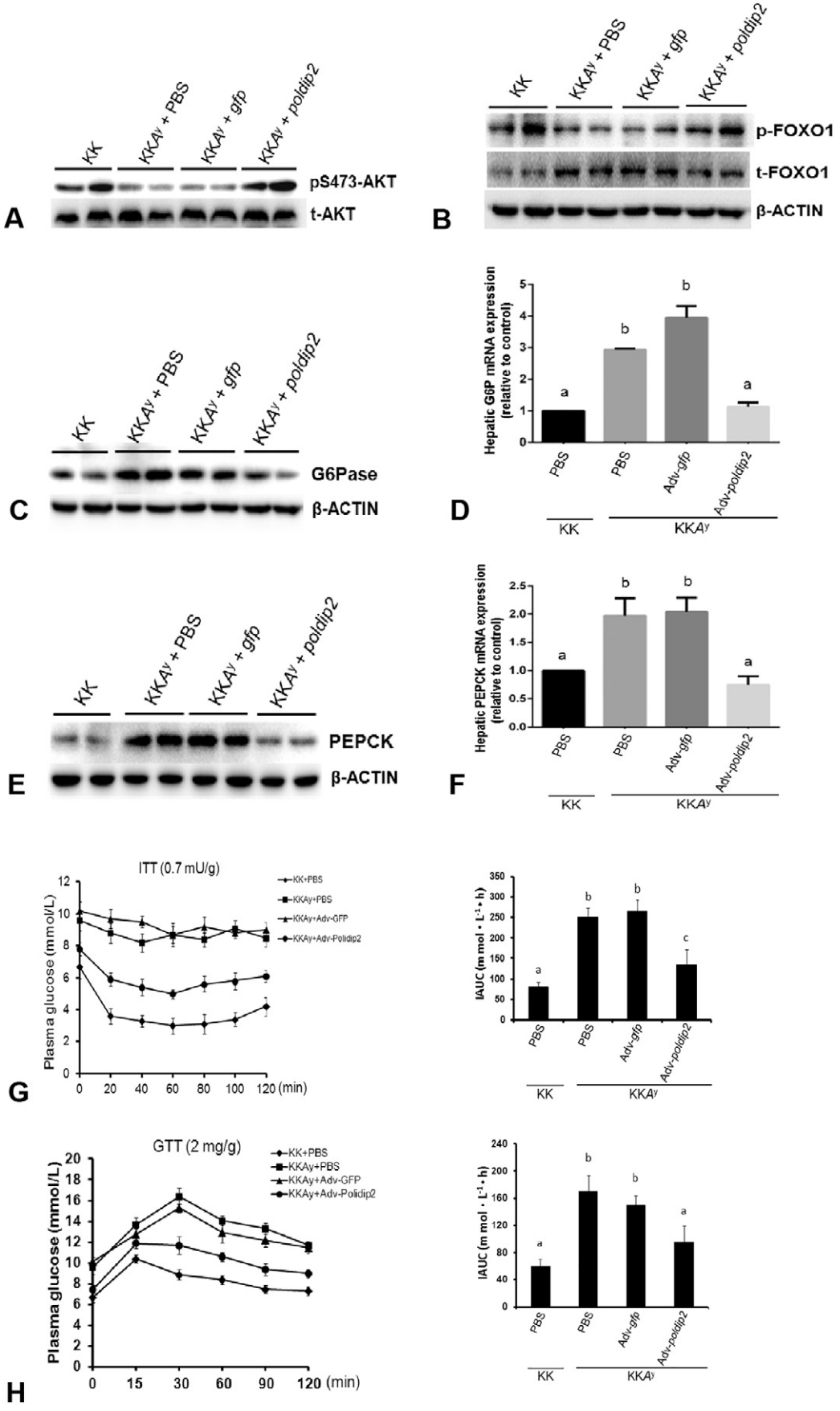
A
KK
KKAy + PBS
KKAy + gfp
KKAy + poldip2
pS473-AKT
t-AKT
B
p-FOXO1
t-FOXO1
β-ACTIN
C
G6Pase
β-ACTIN
D
Hepatic G6P mRNA expression (relative to control)
PBS
Adv-gfp
Adv-poldip2
E
PEPCK
β-ACTIN
F
Hepatic PEPCK mRNA expression (relative to control)
G
ITT (0.7 mU/g)
KK+PBS
KKAy+PBS
KKAy+Adv-GFP
KKAy+Adv-Polidip2
Plasma glucose (mmol/L)
(min)
IAUC (m mol · L-1 · h)
H
GTT (2 mg/g)

[24,26–28]. In the present study, we found that *in vivo* expression of Poldip2 in diabetic livers normalized the phosphorylation levels of Ser473 in AKT enzymes (Fig. 7A), thus resulting in the dramatic enhancement of FoxO1 phosphorylation (Fig. 7B), which led to the exclusion of FoxO1 protein from cellular nucleus. Owing to the suppression of FoxO1 activity, the two key proteins for hepatic gluconeogenesis, G6Pase and PEPCK, were substantially diminished after *in vivo* replenishment of Poldip2 protein in diabetic murine livers (Fig. 7C, E). Meanwhile, the elevated hepatic G6Pase and PEPCK mRNA levels by T2DM were normalized by the *in vivo* expression of Poldip2, as compared to the healthy control mice (Fig. 7D, F). In addition, the ITT and GTT assays showed the marked amelioration of insulin sensitivity caused by the *in vivo* hepatic expression of Poldip2 in T2DM KKA^y mice (Fig. 7G, H). These results are also consistent with the substantial diminishment of plasma glucose levels and with the significant improvement of HOMA-IR after the hepatic restitution of Poldip2 protein in T2DM KKA^y mice (Table 1).

4. Discussion

In type 2 diabetes, the increased supply of energy substrates and the inflammatory environment is thought to elicit the overproduction of mitochondrial ROS that activates protein kinase signaling pathways that suppress the insulin signal downstream of the insulin receptor (IR) at the level of IR substrate-1 (IRS-1) and phosphatidylinositol-3-kinase (PI3K) to promote 'insulin resistance' [15,29,30]. However, the low/moderate levels of H_2O_2 may in fact be required for normal cellular functioning and intracellular signaling. Such physiological H_2O_2 is generated primarily at the plasma membrane and endomembranes by NADP(H) oxidases [15]. Many stimuli including growth factors and hormones can promote the transient generation of H_2O_2 and this has been shown to be essential for optimal tyrosine phosphorylation-dependent signaling *in vitro* [31,32]. Principal targets of H_2O_2 for promoting tyrosine phosphorylation-dependent signaling are the protein tyrosine phosphatases (PTPs), which is consistent with our results in this study.

According to the previous literature, the glucose might generate ROS [33,34]. In current study, we found that high glucose concentration did not elicit the sharp overproduction of ROS, although it raised moderately more ROS than did low glucose in cultured hepatocytes. This may be at least in part due to the relative short time incubation (24 h) of the cells. Interestingly, our data also showed that insulin and leptin exerted the same trend of inhibition for Poldip2 expression in cultured liver cells with high concentration of glucose. This makes sense because leptin and insulin may share some cross links in the signaling pathways [35–37], although they function through different receptors.

In the present study, we found that hepatic inhibition of NOX 4 activity caused by suppression of Poldip2 in T2DM elicited the deficiency of physiological signaling-functional H_2O_2, another disturbance of "redox homeostasis", resulting in the abnormal accumulation of hepatic cholesterol and hypertriglyceridemia. More importantly, the *in vivo* restoration of Poldip2 protein level in murine diabetic livers generated the low/moderate amount of H_2O_2, thereby rescuing the hepatic insulin sensitivity *via* inhibiting the PTPase activity, thus normalizing the hepatic gluconeogenesis and cholesterol production, and improving the hypertriglyceridemia as well. These results suggest that low/moderate H_2O_2 level generated by NOX4 in liver may be essential for normal physiology, and that deficiency of physiological H_2O_2 triggered by the hepatic inhibition of Poldip2 may be one of the causes for pathogenesis of T2DM. Taken together, our current findings may shed a new light on the molecular mechanism underlying the T2DM.

Declaration of Competing Interest

All authors claim no conflict of interests.

Acknowledgements

Chen K and Wan G for experimental design, fund support and manuscript reviewing/editing. Jiang Z, Zhou J, Li T, for experimental data collection and analysis, Tian M, Lu J and Jia Y for reagent preparations.

Funding

This work was supported by the grant from National Natural Science Foundation of China (NSFC, 81570786 to K.C.), intramural fund of Anhui Medical University (to K.C.); and National Key Research and Development Program of China (2018YFA 0107304 and 2017 YFA 0105000 to G.W.); and Wanjiang young scholar grant from Anhui Province of China (9101041203, to Z.J.).

Data and resource availability

All data generated or analyzed during this study are included in the published article and its online supplementary files.

Appendix A. Supplementary data

Supplementary data to this article can be found online at https://doi.org/10.1016/j.metabol.2019.153948.

References

[1] Valko M, Rhodes CJ, Moncol J, Izakovic M, Mazur M. Free radicals, metals and antioxidants in oxidative stress-induced cancer. Chem Biol Interact 2006;160:1–40.
[2] Kovacic P, Jacintho JD. Mechanisms of carcinogenesis: focus on oxidative stress and electron transfer. Curr Med Chem 2001;8:773–96.

Fig. 7. Hepatic expression of *POLDIP2* in diabetic KKA^y mouse livers effectively dampens the gluconeogenesis and significantly improves insulin sensitivity. Type 2 diabetic KKA^y mice were injected with the adenoviral particles containing wild type *POLDIP2* or *gfp* as described in the Methods section and Fig. 4. The proteins were extracted from the livers of four groups of mice. (A) Shown are the phosphorylation levels of threonine residue at AKT protein, a rate-limiting enzyme for insulin signaling, and its total protein levels in the four groups. (B) The same samples as in (A) were assayed again, displayed are the phosphorylation levels of FOXO1, a key downstream target of AKT for regulating hepatic gluconeogenesis, and its total protein levels as loading control. (C) Shown are the immunoblots of G6Pase protein, a key enzyme for hepatic gluconeogenesis, for the same four groups of mice as in (A). (D) After the adenoviral injection in four groups of mice, mRNA levels of G6Pase were measured by qRT-PCR and shown as relative to control β-actin mRNA levels. (Mean ± SEM, $n = 3$), columns labeled with different lower case letters (a, b) are statistically different, $p < 0.001$ (ANOVA). (E) Immunoblots are shown the levels of PEPCK protein, another key enzyme for hepatic gluconeogenesis, for the same four groups of mice as in (A). (F) After the adenoviral injection in four groups of mice, mRNA levels of PEPCK were measured by qRT-PCR and shown as relative to control β-actin mRNA levels. (Mean ± SEM, $n = 3$), columns labeled with different lower case letters (a, b) are statistically different, $p < 0.001$ (ANOVA). (G) After the adenoviral injection in four groups of mice, 6–8 h fasted conscious mice were injected by bovine insulin into the intraperitoneal cavity and glucose in tail blood was immediately assayed at indicated time points and shown as four curves. Meanwhile the areas under curves were measured for four groups of mice. Columns labeled with different lower case letters (a, b, c) are statistically different, $p < 0.01$ (Student-Newman-Keuls test). (H) After the adenoviral injection in four groups of mice, a bolus of glucose was injected into the intraperitoneal cavity and blood was sampled at indicated times. Shown are plasma glucose levels for four groups of mice. Meanwhile the areas under curves were measured. Columns labeled with different lower case letters (a, b, c) are statistically different, $p < 0.01$ (Student-Newman-Keuls test). All data in this figure are representative of three independent experiments, respectively.

[3] Ridnour LA, Isenberg JS, Espey MG, Thomas DD, Roberts DD, Wink DA. Nitric oxide regulates angiogenesis through a functional switch involving thrombospondin-1. Proc Natl Acad Sci U S A 2005;102:13147–52.
[4] Valko M, Morris H, Mazur M, Rapta P, Bilton RF. Oxygen free radical generating mechanisms in the colon: do the semiquinones of Vitamin K play a role in the aetiology of colon cancer? Biochim Biophys Acta 2001;1527:161–6.
[5] Valko M, Leibfritz D, Moncol J, Cronin MT, Mazur M, Telser J. Free radicals and antioxidants in normal physiological functions and human disease. Int J Biochem Cell Biol 2007;39:44–84.
[6] Lambeth JD. Nox enzymes, ROS, and chronic disease: an example of antagonistic pleiotropy. Free Radic Biol Med 2007;43:332–47.
[7] Zorov DB, Juhaszova M, Sollott SJ. Mitochondrial ROS-induced ROS release: an update and review. Biochim Biophys Acta 2006;1757:509–17.
[8] Brown DI, Griendling KK. Nox proteins in signal transduction. Free Radic Biol Med 2009:1239–53.
[9] Bedard K, Krause KH. The NOX family of ROS-generating NADPH oxidases: physiology and pathophysiology. Physiol Rev 2007;87:245–313.
[10] Chen K, Kirber MT, Xiao H, Yang Y, Keaney Jr JF. Regulation of ROS signal transduction by NADPH oxidase 4 localization. J Cell Biol 2008;181:1129–39.
[11] Martyn KD, Frederick LM, von Loehneysen K, Dinauer MC, Knaus UG. Functional analysis of Nox4 reveals unique characteristics compared to other NADPH oxidases. Cell Signal 2006;18:69–82.
[12] Droge W. Free radicals in the physiological control of cell function. Physiol Rev 2002; 82:47–95.
[13] Sies H. Role of metabolic H2O2 generation: redox signaling and oxidative stress. J Biol Chem 2014;289(13):8735–41.
[14] Anderson EJ, Lustig ME, Boyle KE, Woodlief TL, Kane DA, Lin CT, et al. Mitochondrial H2O2 emission and cellular redox state link excess fat intake to insulin resistance in both rodents and humans. J Clin Invest 2009;119(3):573–81.
[15] Veal EA, Day AM, Morgan BA. Hydrogen peroxide sensing and signaling. Mol Cell 2007;26:1–14.
[16] Xiao Q, Luo Z, Pepe AE, Margariti A, Zeng L, Xu Q. Embryonic stem cell differentiation into smooth muscle cells is mediated by Nox4-produced H2O2. Am J Physiol Cell Physiol 2009;296:C711–23.
[17] Paik Y-H, Kim J, Aoyama T, de Minicis S, Bataller R, Brenner DA. Role of NADPH oxidases in liver fibrosis. Antioxid Redox Signal 2014;20(17):2854–72.
[18] Lambeth JD. NOX enzymes and the biology of reactive oxygen. Nat Rev Immunol 2004;4(3):181–9.
[19] Mizrahi A, Berdichevsky Y, Ugolev Y, et al. Assembly of the phagocyte NADPH oxidase complex: chimeric constructs derived from the cytosolic components as tools for exploring structure-function relationships. J Leukoc Biol 2006;79 (5):881–95.
[20] Clempus RE, Sorescu D, Dikalova AE, Pounkova L, Jo P, Sorescu GP, et al. Nox4 is required for maintenance of the differentiated vascular smooth muscle cell phenotype. Arterioscler Thromb Vasc Biol 2007;27:42–8.
[21] Lyle AN, Deshpande NN, Taniyama Y, Seidel-Rogol B, Pounkova L, Du P, et al. Poldip2, a novel regulator of Nox4 and cytoskeletal integrity in vascular smooth muscle cells. Circ Res 2009;105:249–59.
[22] Liu L, Rodriguez-Belmonte E, Mazloum N, Xie B, Lee M. Identification of a novel protein, PDIP38, that interacts with the p50 subunit of DNA polymerase delta and proliferating cell nuclear antigen. J Biol Chem 2003;278:10041–7.
[23] Xie B, Li H, Wang Q, Xie S, Rahmeh A, Dai W, et al. Further characterization of human DNA polymerase delta interacting protein 38. J Biol Chem 2005;280:22375–84.
[24] Wu X, Williams KJ. The NOX4 pathway as a source of selective insulin resistance and responsiveness. Arterioscler Thromb Vasc Biol 2012;32(5):1236–45.
[25] Loh K, Deng H, Fukushima A, Cai X, Boivin B, Galic S, et al. Reactive oxygen species enhance insulin sensitivity. Cell Metab 2009;10(4):260–72.
[26] Wu X, Chen K, Williams KJ. The role of pathway-selective insulin resistance and responsiveness in diabetic dyslipoproteinemia. Curr Opin Lipidol 2012;23:334–44.
[27] Cusi K, Maezono K, Osman A, et al. Insulin resistance differentially affects the PI 3-kinase- and MAP kinase-mediated signaling in human muscle. J Clin Invest 2000; 105:311–20.
[28] Shimomura I, Matsuda M, Hammer RE, et al. Decreased IRS-2 and increased SREBP-1c lead to mixed insulin resistance and sensitivity in livers of lipodystrophic and ob/ob mice. Mol Cell 2000;6:77–86.
[29] Kim JA, Wei Y, Sowers JR. Role of mitochondrial dysfunction in insulin resistance. Circ Res 2008;102:401–14.
[30] Newsholme P, Haber EP, Hirabara SM, Rebelato EL, Procopio J, Morgan D, et al. Diabetes associated cell stress and dysfunction: role of mitochondrial and non-mitochondrial ROS production and activity. J Physiol 2007;583:9–24.
[31] Rhee SG. Cell signaling. H2O2, a necessary evil for cell signaling. Science 2006;312: 1882–3.
[32] Tonks NK. Protein tyrosine phosphatases: from genes, to function, to disease. Nat Rev Mol Cell Biol 2006;7:833–46.
[33] Yu T, Sheu SS, Robotham JL, Yoon Y. Mitochondrial fission mediates high glucose-induced cell death through elevated production of reactive oxygen species. Cardiovasc Res 2008;79:341–51.
[34] Wu N, Shen H, Liu H, Wang Y, Bai Y, Han P. Acute blood glucose fluctuation enhances rat aorta endothelial cell apoptosis, oxidative stress and proinflammatory cytokine expression in vivo. Cardiovasc Diabetol 2016;15(1):109.
[35] Myers Jr MG. Leptin receptor signaling and the regulation of mammalian physiology. Recent Prog Horm Res 2004;59:287–304.
[36] Huang W, Metlakunta A, Dedousis N, Ortmeyer HK, Stefanovic-Racic M, O'Doherty RM. Leptin augments the acute suppressive effects of insulin on hepatic very low-density lipoprotein production in rats. Endocrinology 2009;150:2169–74.
[37] Petersen KF, Oral EA, Dufour S, Befroy D, Ariyan C, Yu C, et al. Leptin reverses insulin resistance and hepatic steatosis in patients with severe lipodystrophy. J Clin Invest 2002;109:1345–50.